

Pretubulysin derived probes as novel tools for monitoring the microtubule network *via* activity-based protein profiling and fluorescence microscopy†

Jürgen Eirich,^a Jens L. Burkhart,^b Angelika Ullrich,^b Georg C. Rudolf,^a Angelika Vollmar,^c Stefan Zahler,^c Uli Kazmaier^b and Stephan A. Sieber^{*a}

Received 13th April 2012, Accepted 18th May 2012

DOI: 10.1039/c2mb25144b

Microtubules (mt) are highly dynamic polymers composed of alpha- and beta-tubulin monomers that are present in all dividing and non-dividing cells. A broad variety of natural products exists that are known to interfere with the microtubule network, by either stabilizing or de-stabilizing these rope-like polymers. Among those tubulysins represent a new and potent class of cytostatic tetrapeptides originating from myxobacteria. Early studies suggested that tubulysins interact with the eukaryotic cytoskeleton by inhibition of tubulin polymerization with EC₅₀ values in the picomolar range. Recently, pretubulysins have been described to retain the high tubulin-degradation activity of their more complex tubulysin relatives and represent an easier synthetic target with an efficient synthesis already in place. Although tubulin has been suggested as the dedicated target of tubulysin a comprehensive molecular target analysis of pretubulysin in the context of the whole proteome has not been carried out so far. Here we utilize synthetic chemistry to develop two pretubulysin photoaffinity probes which were applied in cellular activity-based protein profiling and imaging studies in order to unravel and visualize dedicated targets. Our results clearly show a remarkable selectivity of pretubulysin for beta-tubulin which we independently confirmed by a mass-spectrometry based proteomic profiling platform as well as by tubulin antibody based co-staining on intact cells.

Introduction

Microtubules (mt) are highly dynamic polymers composed of α - and β -tubulin monomers that are present in all dividing and non-dividing cells.^{1,2} These components of the cytoskeleton play a major role in forming the spindle apparatus during mitosis, which was recognized early on as an interesting drug target for selective inhibition of the growth of fast dividing cells, *e.g.* in cancer.^{3–7}

A broad variety of natural products originating from different organisms exists which are known to interfere with the microtubule network, by either stabilizing or de-stabilizing these rope-like polymers already since the 1970s.^{5,6,8,9} Some of them are marketed drugs, in clinical trials or subject to

academic research. In 2000 Sasse *et al.* discovered a new class of cytostatic tetrapeptides originating from myxobacteria termed tubulysins **1** (Fig. 1).¹⁰ These molecules are assembled by hybrid polyketide synthases/non-ribosomal peptide synthetases and consist of one proteinogenic, isoleucine (Ile), and three non-proteinogenic amino acids including *N*-methyl-pipecolic acid (Mep), tubovaline (Tuv) and a chain extended analogue of either phenylalanine or tyrosine called tubu-phenylalanine (Tup) or tubutyrosine (Tut), respectively. Early studies suggested that tubulysins interact with the eukaryotic cytoskeleton by inhibition of tubulin polymerization with EC₅₀ values in the picomolar range.^{10–12} This potency even exceeds that of other tubulin modifiers such as taxol, vinblastine and epothilone by 20- to 100-fold¹³ and consequently rank tubulysins as the most promising lead structures for pharmaceutical application. However, several prerequisites have to be considered in order to initiate a drug development program. First, easy synthetic access for natural product derivatization has to be established in order to investigate structure–activity relationships (SAR) and provide sufficient compound quantities for pharmacological testing. Moreover, although tubulin has been established as the dedicated target, no information about undesired off-targets in eukaryotic cells is available. Previous SAR studies already revealed several positions with increased tolerance for derivatization.^{13–17} One important

^a Center for Integrated Protein Science Munich CIPS^M, Department of Chemistry, Institute of Advanced Studies IAS, Technische Universität München, Lichtenbergstrasse 4, 85747 Garching, Germany

^b Institut für Organische Chemie, Universität des Saarlandes, Im Stadtwald, Geb. C4.2, 66123 Saarbrücken, Germany

^c Department of Pharmacy, Pharmaceutical Biology, Ludwig-Maximilians-Universität München, Butenandtstr. 5-13, 81377 München, Germany

† Electronic supplementary information (ESI) available: Additional fluorescent gel scans, MS data, compound structures and synthesis of trifunctional linkers, synthetic procedures for pretubulysin probes. See DOI: 10.1039/c2mb25144b

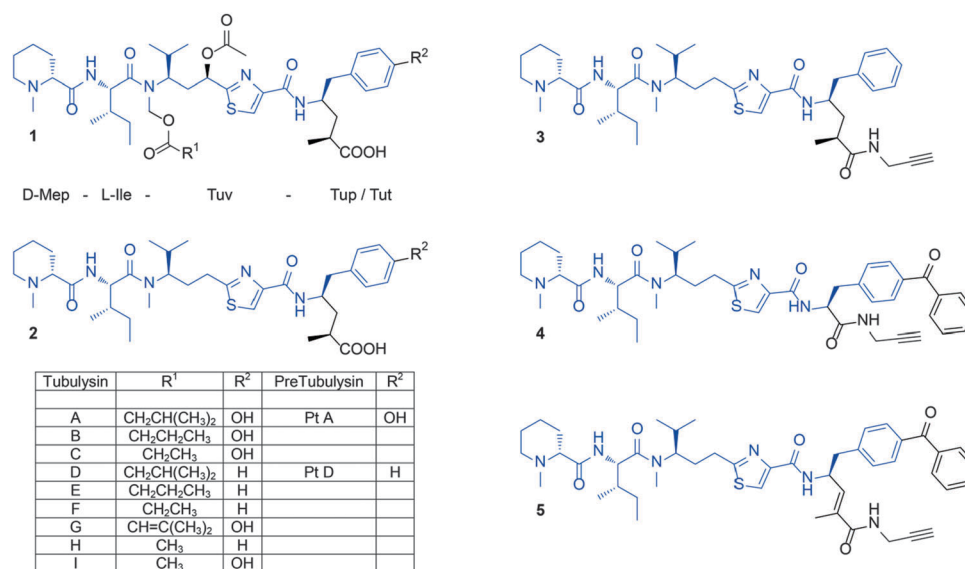


Fig. 1 Probe design – structures of the naturally occurring tubulysins **1** and pretubulysin (Pt) **2** (left) as well as derived probes (Pt propargyl amide **3**, benzophenone probes **4** and **5**) (right) with common core motive indicated in blue.

finding included the replacement of a chemically labile *N,O*-acetal of tubulysin **1** by alkyl groups and the removal of the acetoxy group at the central amino acid tubovaline (Tuv). The resulting chemically less complex compounds are called pretubulysins (Pt) **2** and have been also found in nature as biosynthetic precursors of the tubulysins (Fig. 1).¹⁸ Interestingly, pretubulysins retain the high tubulin-degradation activity of their more complex tubulysin relatives and represent an easier synthetic target with an efficient synthesis already in place.^{13,19} Here we utilize this well-established route to develop two pretubulysin photoaffinity probes **4** and **5** which are applied in cellular activity based protein profiling and imaging studies in order to unravel and visualize dedicated targets (Fig. 2).^{20–24} Our results clearly show a remarkable selectivity of pretubulysin for tubulin which we independently confirmed by a mass-spectrometry based proteomic profiling platform as well as by tubulin antibody based co-staining on intact cells.

Methods and materials

Synthesis

For synthetic details please refer to the ESI.†

Cell culture

The cell lines Hela, H460 and Jurkat were grown in RPMI-1640, A549 in DMEM (high glucose) with 10% FBS in 5% CO₂ at 37 °C. The adherently growing cell lines were detached with trypsin-EDTA.

MTT assay

Cells were grown in 96-well-plates at a concentration of 5000 cells per cavity. After removing the growth medium by suction compounds **2**, **3**, **4** and **5** in 100 μL medium (without FBS) with a final DMSO concentration of 1% were added and the cells incubated for 24 h at 37 °C and 5% CO₂. After 24 h of exposure,

20 μL (5 mg mL⁻¹) filtered MTT stock solution in PBS were added and the medium was mixed by gentle pipetting. The cells were incubated at 37 °C and 5% CO₂ for 1.5 h to allow the MTT to be metabolized and the reaction was controlled under the microscope. Subsequently, the medium was removed and the produced formazan resuspended in 200 μL DMSO by placing the well-plate on a shaking table for 2 min and 650 rpm. The optical density was read out at λ = 570 nm and λ = 630 nm with a Tecan Infinite 200 PRO NanoQuant microplate reader and the background was subtracted at λ = 630 nm. Cells incubated with 1% DMSO served as control. Three independent replicates were conducted.

The EC₅₀ values were determined using the non-linear fit for dose response of OriginPRO 8.5.1.

In vitro analytical labeling experiments

Cells were detached by scraping from the culture dishes. The pellet was homogenized in PBS by sonication with a Bandelin Sonopuls instrument with 5 × 15 s pulsed at 70% max. power under ice cooling. Proteome samples were adjusted to a final concentration of 2 mg protein mL⁻¹ by dilution in PBS prior to probe labeling. The experiments were carried out in 43 μL total volume, such that once click chemistry (CC) reagents were added, a total reaction volume of 50 μL was reached. In the case of competitive displacement experiments Pt was added and the proteomes were preincubated with the compound for 15 min at 22 °C. Reactions were initiated by addition of varying concentrations of probes and allowed to incubate (additionally) for 15 min at 22 °C. Then they were irradiated in open polystyrene micro-well plates for 60 min on ice with 366 nm UV light (Benda UV hand lamp NU-15 W). For heat controls the proteome was denatured with 2% SDS (4 μL of 21.5% SDS) at 95 °C for 6 min and cooled to 22 °C before the probe was applied. Following incubation, 13 μM rhodamine-azide (Rh-N₃) (1 μL) followed by 1 mM TCEP (1 μL) and 100 μM TBTA ligand (3 μL) were added. Samples were gently vortexed

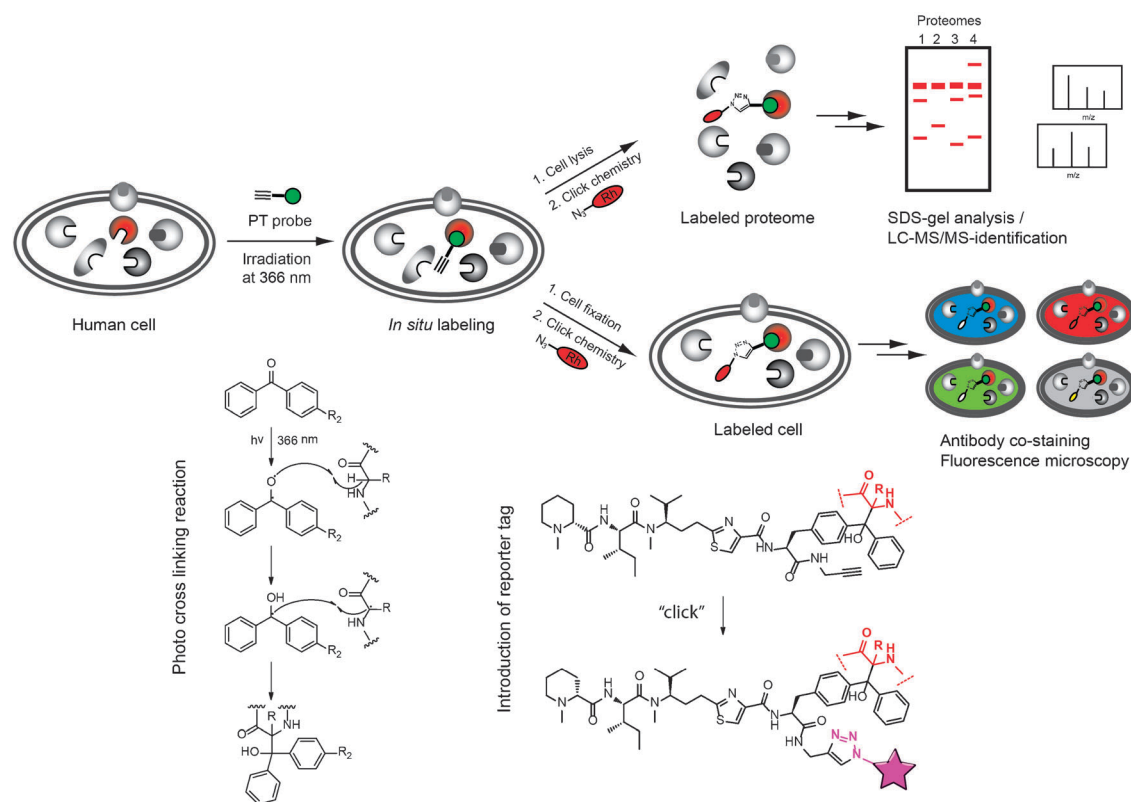


Fig. 2 Experimental design – general labeling procedure with UV-induced cross-link between target protein and probe in living cells (left) enables a broad variety of down-stream applications such as MS based proteomics as well as fluorescence imaging depending on the reporter tag introduced *via* bio-orthogonal click-chemistry (right).

and the cycloaddition was initiated by the addition of 1 mM CuSO_4 (1 μL).

The reaction mixtures were incubated at 22 °C for 1 h. For gel electrophoresis, 50 μL of 2 \times SDS loading buffer was added, and 50 μL applied on the gel. Fluorescence was recorded in a Fujifilm LAS4000 luminescent image analyzer with a Fujinon VRF43LMD3 lens and a 575DF20 filter.

In situ analytical and preparative experiments

For preparative *in situ* studies cells were grown to 80–90% confluence in cell culture petri dishes. After suction and washing with PBS, compound **5** was added in 15 mL medium without FCS and a final DMSO concentration of 0.1%. The cells were incubated with the probe for different periods of time at 37 °C and 5% CO_2 . The medium was removed and the cells were covered with PBS prior to UV irradiation (0 °C, 1 h, 366 nm). The cells were detached with a cell scraper, washed with PBS and the pellet homogenized by sonication. The proteomes were separated into cytosolic and membrane fractions, followed by CC either in 43 μL for analytical ABPP experiments or in a final volume of 1 mL of the proteome sample with 20 μM trifunctional linker (2 μL), 1 mM TCEP (10 μL) and 100 μM TBTA ligand (30 μL) for preparative ABPP. Samples were gently vortexed, and the cycloaddition was initiated by the addition of 1 mM CuSO_4 (10 μL).

Reactions for enrichment were carried out together with a control lacking the probe to compare the results of the biotin-avidin-enriched samples with the background of unspecific

protein binding on avidin-agarose beads. After CC proteins were precipitated using a 5-fold volume of prechilled acetone, samples were stored at –20 °C for 60 min and centrifuged at 16000g for 10 min. The supernatant was discarded and the pellet washed two times with 200 μL of prechilled methanol and resuspended by sonication. Subsequently, the pellet was dissolved in 1 mL of PBS with 0.2% SDS by sonication and incubated under gentle mixing with 50 μL of avidin-agarose beads (Sigma-Aldrich) for 1 h at room temperature. The beads were washed three times with 1 mL of PBS/0.2% SDS, twice with 1 mL of 6 M urea, and three times with 1 mL of PBS. 50 μL of 2 \times SDS loading buffer were added and the proteins were released for preparative SDS-PAGE by 6 min incubation at 95 °C. Gel bands were isolated, washed, and tryptically digested as described previously.³³

Mass spectrometry and bioinformatics

Tryptic peptides were loaded onto a Dionex C18 Nano Trap Column (100 μm) and subsequently eluted and separated by a Dionex C18 PepMap 100 mm (3 μm) column for analysis by tandem MS followed by high-resolution MS using a coupled Dionex Ultimate 3000 LC-Thermo LTQ Orbitrap XL system. The mass spectrometry data were searched using the SEQUEST algorithm against the corresponding databases *via* the software “Proteome Discoverer 1.3”. The search was limited to only tryptic peptides, two missed cleavage sites, monoisotopic precursor ions, and a peptide tolerance of <5 ppm.^{33,41}

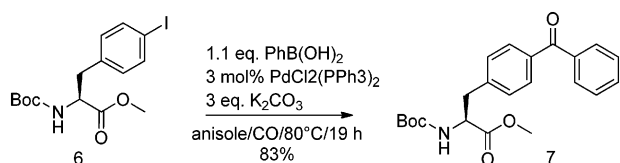
Fluorescence imaging

Hela cells were seeded in carriers compatible with high resolution microscopy (μ -slides, Ibidi). After two days, cells were incubated with the respective pretubulysin derivatives for 1 to 30 min. Subsequently the cells were irradiated (366 nm) at 37 °C (in order to keep the microtubules intact) for 10 min, and then rapidly fixed in methanol (-20 °C). After three washing steps in PBS, cells were incubated for 20 min with a freshly prepared solution containing 775 μ l PBS, 20 μ l CuSO_4 (50 mM), 5 μ l dye-azid (5 mM), and 200 μ l ascorbic acid (500 mM). After three times washing with PBS, the cells were incubated with primary tubulin antibody (1 : 400, abcam rabbit anti α tubulin) for 60 min, washed again three times, and then incubated with a secondary antibody (goat anti rabbit AlexaFluor 488, Invitrogen, 1 : 400) and 1 μ g mL^{-1} HOECHST for nuclear staining for 45 min. After three final washing steps, the samples were mounted with Permafluor (Thermo Scientific) and glass cover slides. The samples were observed on a confocal laser scanning microscope (LSM510 meta, Zeiss) with a 63 \times lens, using a pinhole diameter, which generates optical slices of 1 μ m thickness.

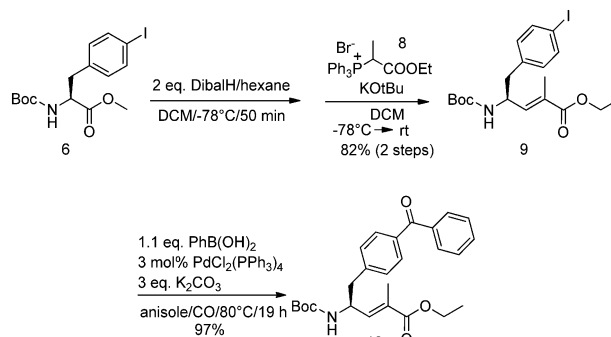
Results and discussion

Chemical probe design and synthesis

One major challenge in the design of photoaffinity probes for target discovery is the introduction of the photolinker as well as the tag which is required as a reporter for protein identification. While the tag is usually a small alkyne moiety that can be modified by post-labeling *via* the Huisgen–Sharpless–Meldal cycloaddition^{25–28} the photolinker is bulky and may cause a steric clash in the active site pocket/binding site of the target protein (Fig. 2).^{29,30} Therefore, a careful chemical design is required in order to incorporate the photolinker in a way that it is at least partially embedded into the compound scaffold. As pretubulysin **2** exhibits a C-terminal tubuphenylalanine (Tup) moiety which can be modified with only little loss of activity according to SAR^{14–17} studies we decided to expand its aromatic system by carbonylative cross coupling to a photoactive benzophenone moiety. In order to assemble the pretubulysin photo-probe we first established a reliable synthetic procedure for the *p*-benzoyl-phenylalanine (pB-Phe) building block (Scheme 1) before the more complex *p*-benzoyl-tubuphenylalanine (pB-Tup) moiety was approached. Carbonylative Suzuki coupling of Boc-*p*-iodophenylalanine methylester (**6**), prepared in three steps according to the literature procedure,³¹ with phenylboronic acid gave the desired product **7** in very good yield (83%). For the synthesis of pB-Tup, **6** was first reduced to the corresponding aldehyde with DibalH and subsequently coupled with Wittig reagent **8** in a one-pot



Scheme 1 Carbonylative cross-coupling leading to pB-Phe **7**.



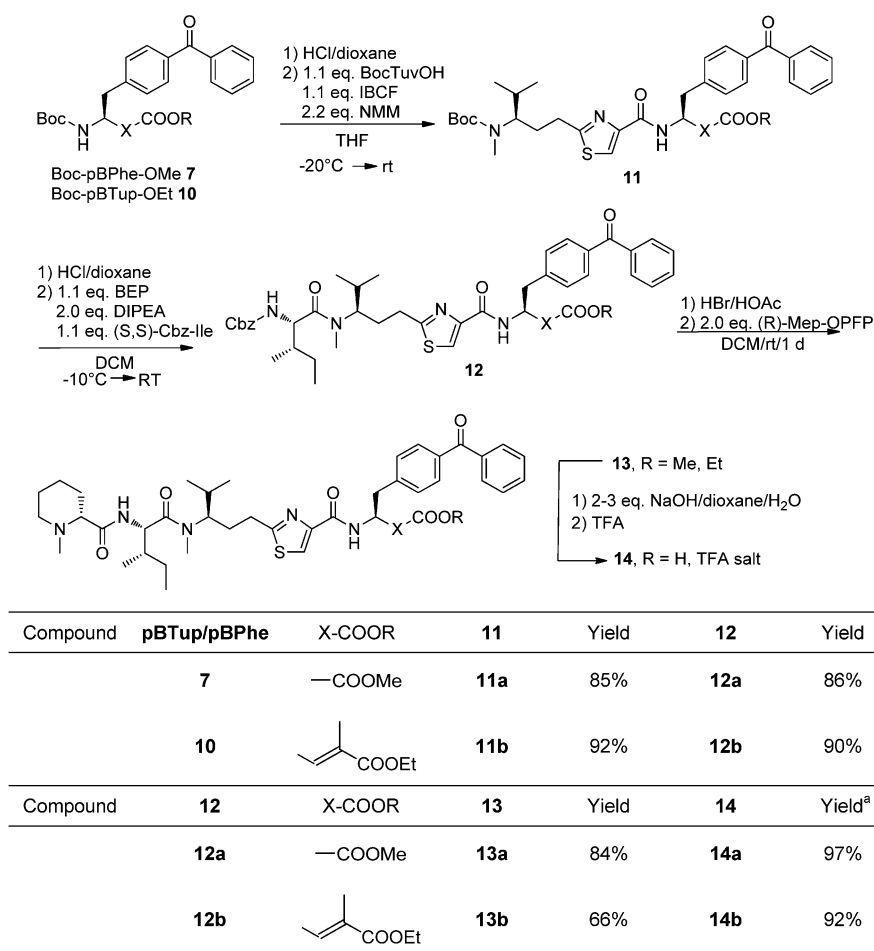
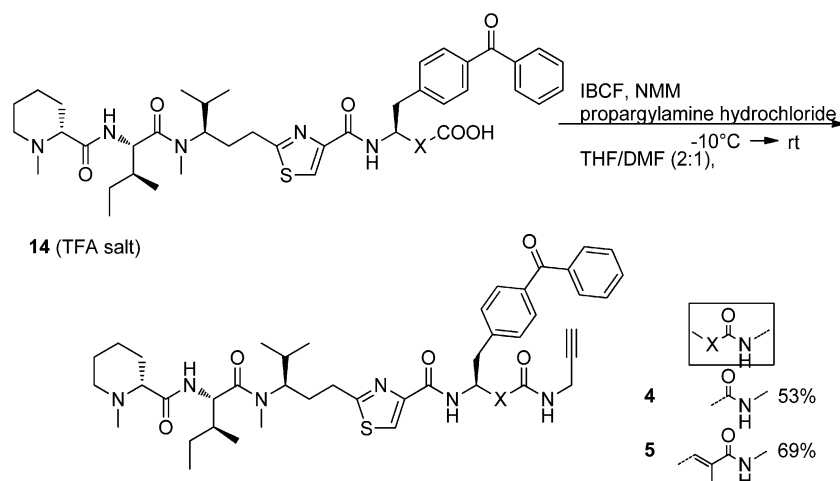
Scheme 2 Synthetic route leading to pB-Tup precursor **10**.

reaction to yield the *p*-iodo-tubuphenylalanine derivative (**9**). This compound was further modified with the above-mentioned carbonylative Suzuki coupling to yield derivative **10** which closely resembles the desired building block with the exception of the double bond that is saturated in the natural product (Scheme 2). All attempts to selectively hydrogenate this bond failed due to the loss of the carbonyl function within the benzophenone moiety. We therefore used the unsaturated precursor building block (**10** – Scheme 2) together with the shorter pB-Phe in order to assemble two structurally different pretubulysin probes **4** and **5**. The synthesis of both probes is outlined in Schemes 3 and 4. In brief, the two benzophenone precursors **7** and **10** were deprotected with HCl in dioxane and subsequently coupled with *N*-Boc-tubu-valine which was activated as a mixed anhydride. The N-terminal tripeptide was prepared according to literature procedures.¹⁸ Subsequent deprotection and coupling with Cbz-(*S,S*)-isoleucine as well as (*R*)-*N*-methyl-pipecolic acid-pentafluorophenyl ester ((*R*)-Mep-OPFP), after Cbz-deprotection, gave the two *N*-methylated tetrapeptides (**13a/b**) in good yields (Scheme 3). In the next step, the methyl, respectively, ethyl ester was saponified with NaOH and the free tetrapeptides were converted to the TFA-salts to get the benzophenone derivatives **14** in excellent yield. Finally, propargylamine was coupled to the C-terminus yielding the desired probes **4** and **5** (Scheme 4).

In order to gain insights into the structure–activity relationship (SAR) of the probe scaffolds we also prepared pretubulysin D (**2**) as well as its C-terminal alkynylated derivative (**3**) as reference compounds according to previous procedures.¹⁸

Bioactivity

Pretubulysin **2** exhibits very potent cytotoxicity against various cell-lines with EC_{50} values in the low nM range (Table 1).^{18,19,32} In order to investigate the effect of structural remodeling on probe potency we tested all three derivatives against various cell lines and obtained a significant drop in potency for probes **4** and **5**. The bioactivity of alkynylated derivative **3** was significantly better compared to the photo-probes emphasizing a higher tolerance for small modifications at the C-terminus. Although the introduction of the additional benzoyl moiety at the phenyl ring of tubuphenylalanine represented the least structural perturbation in order to gain access to benzophenone possible, the drop in potency indicated that this position is quite sensitive for alterations. Nevertheless, the obtained

^aisolated as TFA salt**Scheme 3** Reactions leading to cross-linkable Pt derivatives **14** with deprotected C-terminus.**Scheme 4** Final amide coupling reaction to introduce alkyne tag yielding desired probes **4** and **5**.

EC₅₀s of 8–13 μM for both probes still reflect elevated cytotoxicities with an unresolved mechanism of action. Since all results of cellular profiling will be validated with the unmodified natural product, *e.g.* in competitive profiling experiments (see below), the probes represent suitable tools and a promising starting point for target discovery.

Pretubulysin target analysis

With the tool compounds in hand we next analyzed the cellular target(s) that are responsible for the observed cytotoxicity. Both probes were incubated for 1 h with intact HeLa cells under *in situ* conditions (Experimental section) and

Table 1 EC₅₀ values for compounds **2**, **3**, **4** and **5** determined *via* MTT (24 h incubation time) in four different cell lines

Cell line	Compound/ μM			
	2 (Pt)	3	4	5
Hela	0.02	1.2	7.9	13.4
H460	0.02	1.0	8.1	9.6
Jurkat	<0.01	0.5	8.5	9.2
A549	3.9	40	27	43

irradiated for 1 h at 360 nm in order to establish a covalent link between the probe molecule and all bound proteins.³³ Cells were lysed by sonication and cytosolic as well as membrane fractions separated by centrifugation. Subsequent CC with a fluorescent rhodamine-azide tag followed by SDS polyacrylamide gel separation and fluorescent scanning revealed distinct bands that varied in intensity depending on the applied probe concentration (Fig. 3 and Fig. S1, ESI[†]).^{34–36} While 500 μM , the highest concentration applied, led to the labeling of several proteins, a gradual reduction of probe concentration down to 1–10 μM significantly reduced the number of protein bands. One intense band with a molecular weight of about 60 kDa was labeled under all probe concentrations applied emphasizing a significant specificity and affinity of the probes for this protein target. Contrarily, labeling of this band disappeared when the Hela cell lysate was first denatured by heat treatment and subsequently labeled by the probe emphasizing a specific interaction between the folded

protein and the probe (Fig. S2, ESI[†]). A comparison of both concentration dependent labeling experiments suggests that probe **4** with the shorter C-terminal end exhibits a more pronounced selectivity for the above-mentioned protein target compared to probe **5** (Fig. S3, ESI[†]). Based on the better labeling profile as well as the slightly higher cytotoxicity we conducted all subsequent labeling experiments with probe **4**. In order to evaluate the optimal pre-incubation time probe **4** was incubated with intact Hela cells for several durations ranging from 5 to 120 min. Subsequent irradiation for 1 h and in gel fluorescent scanning revealed that 60 min were already sufficient for effective labeling (Fig. S4, ESI[†]).

In order to evaluate which of the labeled protein bands in Hela cells correspond to pretubulysin binding, we added the unmodified natural product in varying excess to intact cells followed by the probe and applied the standard irradiation labeling procedure. Interestingly, a 4-fold excess of pretubulysin was already sufficient to totally block the labeling of the prominent 60 kDa band which emphasizes a high affinity of the unmodified natural product for the protein binding site. Profiling of several other cell lines including H460, Jurkat and A549 with probe **4** at a concentration close to the EC₅₀ (10 μM) revealed an intense protein band at the same molecular weight as the one observed in Hela emphasizing that the target is highly conserved throughout the different cell lines.

To reveal the identity of this protein band we utilized a proteomic enrichment strategy and incubated Hela cells with

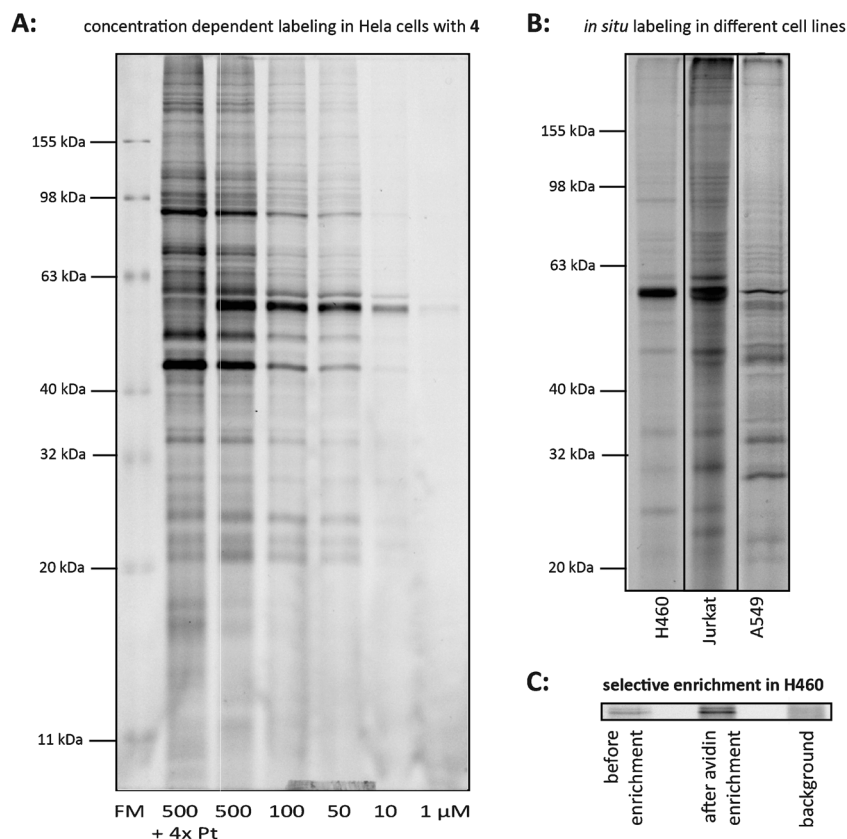


Fig. 3 Fluorescence scans of the *in situ* labeling in Hela cells with probe **4** (1–500 μM) in competition with Pt **2** (2 mM) (**A**) and in comparison with other cell lines (10 μM **4**) (**B**), selective enrichment of tubulin in H460 (5 μM **4**) (**C**).

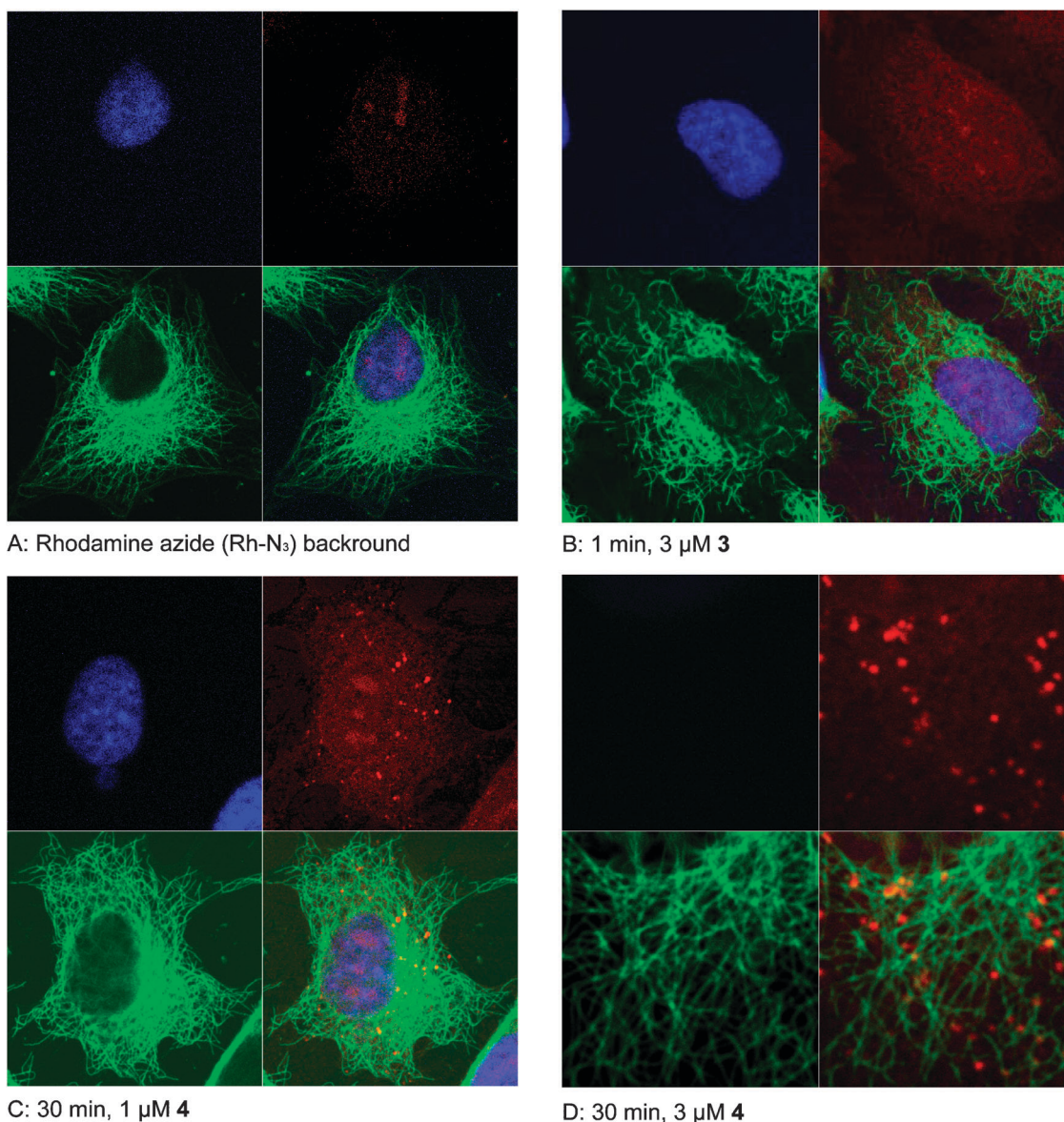


Fig. 4 Fluorescent microscopy: A–D: top left – blue Hoechst, top right – red Rh-N₃, bottom left – green Antibody-Alexa488-conjugate, bottom right – overlay. Probe treatment of cells indicated individually.

probe **4** followed by irradiation, lysis and CC in order to attach a trifunctional rhodamine-biotin-azide tag (ESI[†]).³³ The labeled protein was selectively enriched by binding to avidin beads and separated on a SDS gel after heat cleavage (Fig. 3c). The enriched band was isolated, washed, tryptically digested and subject to mass spectrometric analysis. Peptide fragments were analyzed *via* the proteome discoverer software with the SEQUEST search algorithm. All experiments were carried out with a control in which no probe was added in order to subtract proteins that bind unspecifically to avidin. All experiments conclusively revealed tubulin as the primary target of the probes (Table S1, ESI[†]). While inhibition of tubulin polymerization by tubulysin has been shown in *in vitro* assays previously,^{10–12,37} it is an important result that the structurally less complex precursor pretubulysin also interacts specifically with tubulin explaining its potent bioactivity. Although our probes are significantly less potent compared

to the unmodified natural product, competitive labeling demonstrates that pretubulysin specifically binds to tubulin with high affinity. However, based on our ABPP experiments we cannot exclude that other pretubulysin targets may exist which are not detectable by our probes. Due to the restrictions of ABPP, *e.g.* photocrosslinker, this problem cannot be easily resolved. Since tubulin represents at least a major target of pretubulysin which was detected for the first time *via* full proteome analysis we will focus on this protein and study the cellular effect of tubulin binding in more detail.

Fluorescence imaging

Besides target identification another advantage of the probe molecules is their utility in imaging studies which is suitable to independently confirm the target and reveal insights into

the function and possible effects of binding. We therefore incubated living Hela cells with various concentrations of probe **4**, irradiated the cells to covalently attach the molecule to the target protein and subsequently fixed the cells with methanol after different time points ranging from 1 to 30 min. Fixed cells were reacted with CC reagents (rhodamine-azide, ascorbic acid, ligand and CuSO₄), Hoechst DNA stain as well as tubulin antibodies for the visualization of the probe, the nucleus as well as microtubuli, respectively. A control experiment without the probe but in the presence of CC reagents revealed low background binding of the rhodamine dye which is mandatory for the visualization of specific binding partners (Fig. 4a). While these pretubulysin untreated cells reveal a tight mesh of microtubuli, a 1 min incubation of 3 μ M probe **3** already initiates significant damage of the filament assembly (Fig. 4b). Interestingly, the same phenotype has been reported for pretubulysin previously^{38–40} but so far the direct binding to tubulin could not be directly confirmed. Here we demonstrate by co-staining with the tubulin directed antibody as well as the fluorescent probe that pretubulysin derivative **4** binds to monomeric tubulin which appear as little spots in the image (Fig. 4c and d). The sequestration of tubulin monomers prevents the filament assembly and explains its time dependent dissolution. The results of all imaging experiments are in line with our MS based target analysis and demonstrate that monomeric tubulin is the point of pretubulysin attachment leading to inhibition of filament assembly and subsequent cell death.

From a chemical biology perspective photocrosslinking probe **4** revealed superior imaging properties over compound **3** that lacks the photoreactive moiety. Although compound **3** exhibited a stronger effect on microtubule assembly, the reversible binding was not stable enough to survive the washing procedures. Since photo-linkage is mandatory for the visualization of pretubulysin binding, a next generation of photocrosslinking probes should focus on the introduction of smaller linker moieties such as diazirines in order to maintain the original potency.

In conclusion we designed and synthesized customized pretubulysin probes that revealed tubulin as the main target in living human cells. Although the introduction of the photocrosslinking moiety reduced the biological potency, competitive labeling studies revealed that beta tubulin is the dedicated binding partner of the unmodified natural product. Moreover, the application of both probes at concentrations close to their EC₅₀ value (10 μ M) revealed only beta tubulin as the predominant target emphasizing that this interaction is solely responsible for cell toxicity of these molecules. However, we cannot exclude that additional targets of pretubulysin may exist that could not be identified here due to the steric bulk of the photolinker. The results obtained in this study demonstrate the utility of our approach to identify tubulin as the main target within living cells of different origins as well as to monitor tubulin binding in cells and its associated inhibition of microtubuli assembly.

Acknowledgements

J.E., G.C.R. and S.A.S. thank Mona Wolff for excellent support and Matthew Nodwell for comments on the manuscript.

J.E. was supported by the Deutsche Forschungsgemeinschaft (DFG) FOR1406. G.C.R. was supported by an ERC starting grant. J.E. and G.C.R. were supported by the TUM Graduate School (Faculty Center Chemistry). J.L.B., A.U., A.M.V., S.Z. and U.K. were supported by the DFG FOR1406. S.A.S. was supported by the DFG Emmy Noether, SFB749 and FOR1406, an ERC starting grant and the Center for Integrated Protein Science Munich CIPS^M.

References

- 1 J. B. Olmsted and G. G. Borisy, *Biochemistry*, 1973, **12**, 4282–4289.
- 2 J. B. Olmsted and G. G. Borisy, *Annu. Rev. Biochem.*, 1973, **42**, 507–540.
- 3 C. Dumontet and M. A. Jordan, *Nat. Rev. Drug Discovery*, 2010, **9**, 790–803.
- 4 L. Wilson and M. A. Jordan, *J. Chemother. (Firenze, Italy)*, 2004, **16**(Suppl. 4), 83–85.
- 5 R. A. Stanton, K. M. Gernert, J. H. Nettles and R. Aneja, *Med. Res. Rev.*, 2011, **31**, 443–481.
- 6 A. Jordan, J. A. Hadfield, N. J. Lawrence and A. T. McGown, *Med. Res. Rev.*, 1998, **18**, 259–296.
- 7 P. Giannakakou, D. Sackett and T. Fojo, *J. Natl. Cancer Inst.*, 2000, **92**, 182–183.
- 8 P. B. Schiff, J. Fant and S. B. Horwitz, *Nature*, 1979, **277**, 665–667.
- 9 M. C. Wani, H. L. Taylor, M. E. Wall, P. Coggon and A. T. McPhail, *J. Am. Chem. Soc.*, 1971, **93**, 2325–2327.
- 10 F. Sasse, H. Steinmetz, J. Heil, G. Hofle and H. Reichenbach, *J. Antibiot.*, 2000, **53**, 879–885.
- 11 M. W. Khalil, F. Sasse, H. Lunsdorf, Y. A. Elnakady and H. Reichenbach, *ChemBioChem*, 2006, **7**, 678–683.
- 12 H. Steinmetz, N. Glaser, E. Herdtweck, F. Sasse, H. Reichenbach and G. Hofle, *Angew. Chem., Int. Ed.*, 2004, **43**, 4888–4892.
- 13 A. Ullrich, Y. Chai, D. Pistorius, Y. A. Elnakady, J. E. Herrmann, K. J. Weissman, U. Kazmaier and R. Muller, *Angew. Chem., Int. Ed.*, 2009, **48**, 4422–4425.
- 14 R. Balasubramanian, B. Raghavan, J. C. Steele, D. L. Sackett and R. A. Fecik, *Bioorg. Med. Chem. Lett.*, 2008, **18**, 2996–2999.
- 15 B. Raghavan, R. Balasubramanian, J. C. Steele, D. L. Sackett and R. A. Fecik, *J. Med. Chem.*, 2008, **51**, 1530–1533.
- 16 P. Wipf and Z. Y. Wang, *Org. Lett.*, 2007, **9**, 1605–1607.
- 17 A. W. Patterson, H. M. Peltier and J. A. Ellman, *J. Org. Chem.*, 2008, **73**, 4362–4369.
- 18 (a) A. Ullrich, J. Herrmann, R. Muller and U. Kazmaier, *Eur. J. Org. Chem.*, 2009, 6367–6378; (b) J. Herrmann, Y. A. Elnakady, R. M. Wiedmann, A. Ullrich, M. Rohde, U. Kazmaier, A. M. Vollmar and R. Muller, *PLoS ONE*, 2012, DOI: 10.1371/journal.pone.0037416, accepted manuscript.
- 19 J. L. Burkhart, R. Muller and U. Kazmaier, *Eur. J. Org. Chem.*, 2011, 3050–3059.
- 20 B. F. Cravatt and E. J. Sorensen, *Curr. Opin. Chem. Biol.*, 2000, **4**, 663–668.
- 21 M. J. Evans, A. Saghatelian, E. J. Sorensen and B. F. Cravatt, *Nat. Biotechnol.*, 2005, **23**, 1303–1307.
- 22 M. J. Evans and B. F. Cravatt, *Chem. Rev.*, 2006, **106**, 3279–3301.
- 23 T. Böttcher, M. Pitscheider and S. A. Sieber, *Angew. Chem., Int. Ed.*, 2010, **49**, 2680–2698.
- 24 M. Fonovic and M. Bogoy, *Expert Rev. Proteomics*, 2008, **5**, 721–730.
- 25 R. Huisgen, *1,3 Dipolar Cycloaddition Chemistry*, Wiley, New York, 1984.
- 26 V. V. Rostovtsev, J. G. Green, V. V. Fokin and K. B. Sharpless, *Angew. Chem., Int. Ed.*, 2002, **41**, 2596–2599.
- 27 Q. Wang, T. R. Chan, R. Hilgraf, V. V. Fokin, K. B. Sharpless and M. G. Finn, *J. Am. Chem. Soc.*, 2003, **125**, 3192–3193.
- 28 C. W. Tornøe, C. Christensen and M. Meldal, *J. Org. Chem.*, 2002, **67**, 3057–3064.
- 29 Y. Tanaka, M. R. Bond and J. J. Kohler, *Mol. Biosyst.*, 2008, **4**, 473–480.
- 30 M. B. Nodwell and S. A. Sieber, *Top. Curr. Chem.*, 2011, 1–42.

- 31 H. Y. Lei, M. S. Stoakes, K. P. B. Herath, J. H. Lee and A. W. Schwabacher, *J. Org. Chem.*, 1994, **59**, 4206–4210.
- 32 A. Ullrich, Y. Chai, D. Pistorius, Y. A. Elnakady, J. E. Herrmann, K. J. Weissman, U. Kazmaier and R. Muller, *Angew. Chem., Int. Ed.*, 2009, **48**, 4422–4425.
- 33 J. Eirich, R. Orth and S. A. Sieber, *J. Am. Chem. Soc.*, 2011, **133**, 12144–12153.
- 34 A. E. Speers, G. C. Adam and B. F. Cravatt, *J. Am. Chem. Soc.*, 2003, **125**, 4686–4687.
- 35 A. E. Speers and B. F. Cravatt, *ChemBioChem*, 2004, **5**, 41–47.
- 36 A. E. Speers and B. F. Cravatt, *Chem. Biol.*, 2004, **11**, 535–546.
- 37 Y. A. Elnakady, F. Sasse, H. Lunsdorf and H. Reichenbach, *Biochem. Pharmacol.*, 2004, **67**, 927–935.
- 38 S. Rath, R. Furst, A. Ullrich, J. Burkhardt, A. M. Vollmar, U. Kazmaier and S. Zahler, *Naunyn—Schmiedeberg's Arch. Pharmacol.*, 2011, **383**, 28–28.
- 39 V. Kretzschmann, A. Ullrich, S. Zahler, A. M. Vollmar, U. Kazmaier and R. Furst, *J. Vasc. Res.*, 2011, **48**, 113–113.
- 40 S. Rath, A. Ullrich, J. L. Burkhardt, J. Herrmann, M. Günther, U. Kazmaier, A. M. Vollmar, J. Liebl, R. Fürst and S. Zahler, *J. Vasc. Res.*, 2011, **48**, 231–231.
- 41 T. Böttcher and S. A. Sieber, *Angew. Chem., Int. Ed.*, 2008, **47**, 4600–4603.